Host's guardian protein counters degenerative symbiont evolution

Ryuichi Koga[a,1,2], Masahiko Tanahashi[a,b,1], Naruo Nikoh[c], Takahiro Hosokawa[d], Xian-Ying Meng[a], Minoru Moriyama[a], and Takema Fukatsu[a,e,f,2]

[a]Bioproduction Research Institute, National Institute of Advanced Industrial Science and Technology, 305-8566 Tsukuba, Japan; [b]Department of Life Science, National Taiwan Normal University, 116 Taipei, Taiwan; [c]Department of Liberal Arts, The Open University of Japan, 261-8586 Chiba, Japan; [d]Department of Biology, Faculty of Science, Kyushu University, 812-8581 Fukuoka, Japan; [e]Department of Biological Sciences, The University of Tokyo, 113-0033 Tokyo, Japan; and [f]Graduate School of Life and Environmental Sciences, University of Tsukuba, 305-8572 Tsukuba, Japan

Edited by Nancy A. Moran, the University of Texas at Austin, Austin, TX, and approved May 11, 2021 (received for review February 28, 2021)

Microbial symbioses significantly contribute to diverse organisms, where long-lasting associations tend to result in symbiont genome erosion, uncultivability, extinction, and replacement. How such inherently deteriorating symbiosis can be harnessed to stable partnership is of general evolutionary interest. Here, we report the discovery of a host protein essential for sustaining symbiosis. Plataspid stinkbugs obligatorily host an uncultivable and genome-reduced gut symbiont, *Ishikawaella*. Upon oviposition, females deposit "capsules" for symbiont delivery to offspring. Within the capsules, the fragile symbiotic bacteria survive the harsh conditions outside the host until acquired by newborn nymphs to establish vertical transmission. We identified a single protein dominating the capsule content, which is massively secreted by female-specific intestinal organs, embedding the symbiont cells, and packaged into the capsules. Knockdown of the protein resulted in symbiont degeneration, arrested capsule production, symbiont transmission failure, and retarded nymphal growth, unveiling its essential function for ensuring symbiont survival and vertical transmission. The protein originated from a lineage of odorant-binding protein-like multigene family, shedding light on the origin of evolutionary novelty regarding symbiosis. Experimental suppression of capsule production extended the female's lifespan, uncovering a substantial cost for maintaining symbiosis. In addition to the host's guardian protein, the symbiont's molecular chaperone, GroEL, was overproduced in the capsules, highlighting that the symbiont's eroding functionality is compensated for by stabilizer molecules of host and symbiont origins. Our finding provides insight into how intimate host–symbiont associations can be maintained over evolutionary time despite the symbiont's potential vulnerability to degeneration and malfunctioning.

symbiont capsule | host secretion protein | vertical transmission | odorant-binding protein | symbiont preservation

Microbial symbioses are ubiquitously found in nature, intricately interwoven into the adaptation, ecology, and evolution of almost all life forms (1, 2). In diverse animals encompassing invertebrates and vertebrates, specific microorganisms are present on their body surface, in their alimentary tract, within their body cavity, or even inside their cells (3). In obligate and long-lasting host–symbiont associations, the symbiont genomes often exhibit drastic size reduction and massive gene losses, which are attributed to relaxed natural selection acting on many symbiont genes unnecessary for the intrahost life as well as to irreversibly accumulated deleterious mutations due to strong population bottleneck and restricted horizontal gene acquisitions imposed by continuous vertical transmission (4, 5). Due to the accumulated genetic load, such degenerative symbionts should suffer cellular malfunctioning and instability, which would finally lead to symbiont genome erosion, uncultivability, extinction, and/or replacement (4–7). In this context, both host and symbiont are expected to evolve some molecular mechanisms for stabilizing the symbiotic association that is inherently vulnerable to degeneration and malfunctioning. For the symbiont side, many genome-reduced endosymbiotic bacteria were reported to overproduce molecular capacitors such as heat shock proteins and molecular chaperones, thereby stabilizing molecular structure and functioning of the degenerative bacterial cells (8–10). For the host side, by contrast, little has been known about such molecular mechanisms underpinning the stability of symbiosis. Here, we report the discovery of such a key molecule essential for sustaining symbiosis.

Results and Discussion

Survival of Genome-Eroded Symbiont in Mother-Made Capsules. Stinkbugs of the family Plataspidae host an uncultivable, genome-reduced (~0.7 Mb), and nutrition-provisioning (=essential amino acids) bacterial symbiont *Ishikawaella* in a specialized region of the midgut (11–13). Upon oviposition, adult females deposit "symbiont capsules," each containing around 10^8 *Ishikawaella* cells (14, 15), with eggs on plant surfaces (Fig. 1 *A* and *B*), where the symbiont capsules are exposed to intense sunshine for 7 to 10 d until the eggs hatch and the newborn nymphs orally acquire the symbiont (12, 15). Here, it should be noted that *Ishikawaella* cells must be fragile because, like the 0.6 Mb reduced genome of the aphid endosymbiont *Buchnera* (11, 16), the *Ishikawaella* genome is devoid of major cell wall–related genes. How such a genome-reduced symbiont can survive the harsh

Significance

When laying eggs, plataspid stinkbugs deposit small packets called "symbiont capsules." Newborn stinkbugs suck the capsules to acquire a bacterial mutualist. Without the symbiont, the babies cannot grow and die. Due to the long-lasting symbiosis, the symbiont has experienced genome reduction and become uncultivable. Within the capsules, however, the symbiont can survive for over a week outside the host. Why and how? Here, we uncover a molecular secret implemented in the symbiont capsules. Mother stinkbugs massively produce a special intestinal secretion protein, PMDP, at the expense of their own survival. PMDP embeds the fragile symbiont cells and protects them within the capsules. The host-provisioned molecule for sustaining symbiosis may be utilized for cultivation and/or preservation of fastidious microorganisms.

Author contributions: R.K., M.T., and T.F. designed research; R.K., M.T., N.N., T.H., X.-Y.M., and M.M. performed research; R.K., M.T., N.N., and M.M. analyzed data; and T.F. wrote the paper.

The authors declare no competing interest.

This article is a PNAS Direct Submission.

See online for related content such as Commentaries.

[1]R.K. and M.T. contributed equally to this work.

[2]To whom correspondence may be addressed. Email: r-koga@aist.go.jp or t-fukatsu@aist.go.jp.

This article contains supporting information online at https://www.pnas.org/lookup/suppl/doi:10.1073/pnas.2103957118/-/DCSupplemental.

Published June 14, 2021.

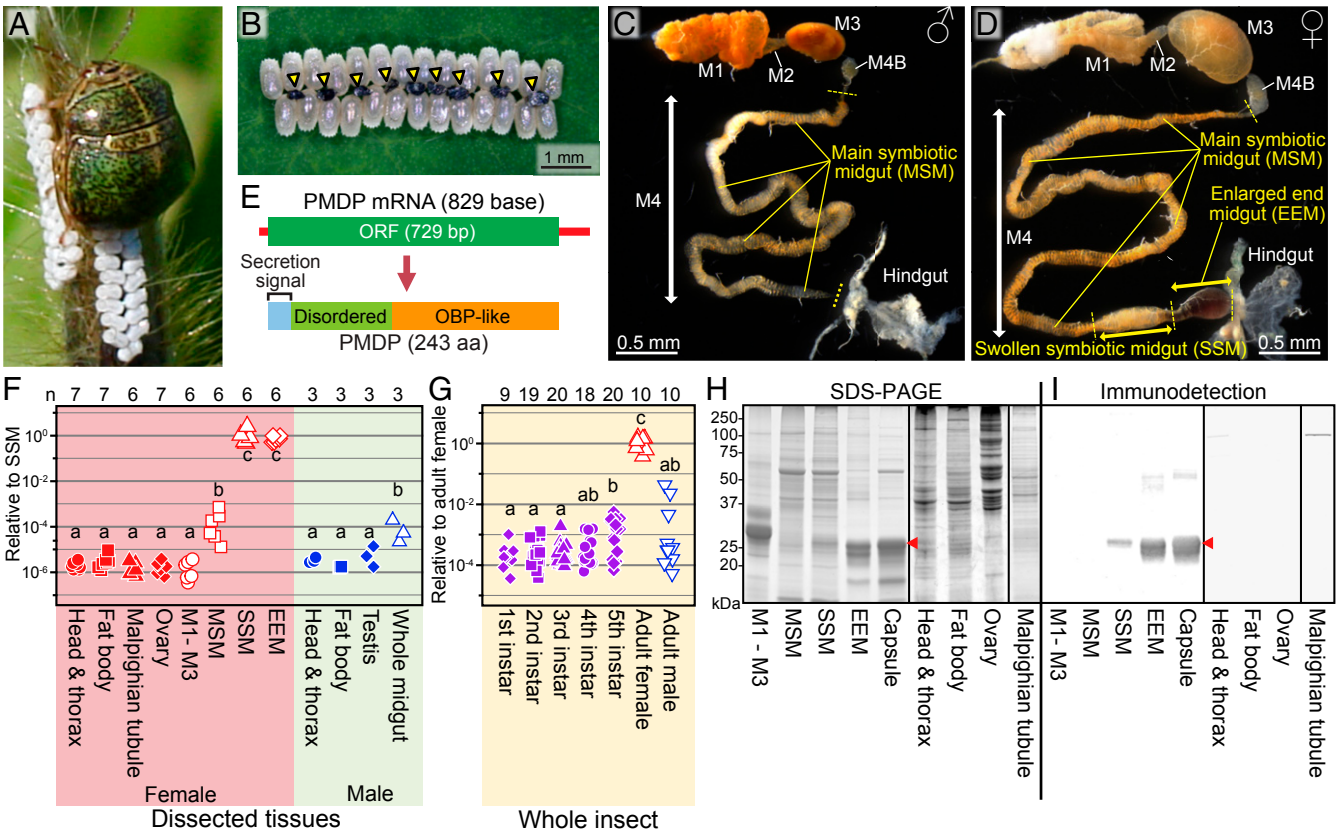

Fig. 1. Gut symbiotic system of *M. punctatissima* and PMDP. (*A*) An adult female of *M. punctatissima* laying eggs on a host plant bud. (*B*) Underside view of an egg mass. Yellow arrowheads indicate symbiont capsules. (*C* and *D*) Dissected alimentary tracts of adult male (*C*) and female (*D*). (*E*) Gene and structure of PMDP. (*F* and *G*) Expression levels of PMDP in dissected tissues (*F*) and in whole insects at different developmental stages (*G*). Values of PMDP complementary DNA (cDNA) copies per Rpl19 cDNA copy obtained by qPCR are regarded as relative expression levels of PMDP gene. For dissected tissues, the average value for SSM is shown as 1, whereas for whole insects, the average value for adult females is shown as 1. The number on the top indicates the number of samples analyzed. Different alphabetical letters (a, b, and c) indicate statistically significant differences (Tukey honestly significant difference [HSD] test: $P < 0.05$). (*H* and *I*) SDS-PAGE of whole proteins (*H*) and immunoblot detection of PMDP (*I*) from dissected tissues of adult females. Red arrowheads indicate PMDP bands. M1, midgut first section; M2, midgut second section; M3, midgut third section; M4, midgut fourth section with crypts (=symbiotic midgut); M4B, M4 bulb.

and fluctuating environment outside the host and successfully establish transmission to the next generation is mysterious.

In plataspid and other stinkbugs, their alimentally tract is differentiated into structurally distinct regions, of which the posterior M4 region is specialized for hosting symbiotic bacteria (17, 18) (Fig. 1*C*). In adult females of plataspid stinkbugs, notably, the voluminous M4 region was further differentiated into specialized sections: main symbiotic midgut (MSM), a long stretch of symbiotic region full of *Ishikawaella*; swollen symbiotic midgut (SSM), a conspicuously thickened symbiotic region; and enlarged end midgut (EEM), a dark-colored enlarged region (Fig. 1*D*). Previous studies regarded these midgut regions as female-specific, capsule-producing organs (12–14), but it has been unknown what genes and molecules are functioning there.

A Single Host Protein, Posterior Midgut Dominant Protein, Predominant in Symbiont Capsules. We performed RNA sequencing of these midgut regions and found that the majority of transcripts represented a single gene in the female-specific regions SSM and EEM in all plataspid species we examined (*SI Appendix*, Table S1). In *Megacopta punctatissima*, for example, the transcript was 829 bp in size, contained a 729-bp open-reading frame, and encoded a protein of 243 amino acid residues, in which the following domains were identified: a secretion signal sequence at the N terminus, an intrinsically disordered region with no predicted stable secondary structure, and an odorant-binding protein (OBP)-like domain at the C terminus with sequence similarity to OBPs of various insects (Fig. 1*E*). qRT-PCR confirmed highly specific and predominant expression of the gene in SSM and EEM of adult females (Fig. 1 *F* and *G*). Sodium dodecyl sulfate polyacrylamide gel electrophoresis (SDS-PAGE) and immunoblotting detected a 28-kDa predominant protein band specifically in SSM, EEM, and symbiont capsules (Fig. 1 *H* and *I* and *SI Appendix*, Fig. S1*A*). Liquid chromatography-mass spectrometry (LC-MS), Southern blotting, and qPCR verified that the 28-kDa protein is derived from the gene that is single copy in the insect genome (*SI Appendix*, Fig. S1 *B–D*). The protein accounted for the majority of total proteins in the symbiont capsules (Fig. 1*H* and *SI Appendix*, Fig. S1), which is hereafter referred to as posterior midgut dominant protein (PMDP). Here, we note that, besides the host-derived PMDP, the symbiont-derived molecular chaperone GroEL was the second most abundant protein in the symbiont capsules (*SI Appendix*, Fig. S1*E*), whose extreme overproduction has been observed in many genome-reduced endosymbiotic bacteria for stabilizing degenerative protein structure and functioning (8, 10).

Symbiont Cells Embedded in PMDP and Packaged into Capsules. We histologically investigated the detailed processes of capsule formation in the female-specific midgut organs, which uncovered structural and functional specialization of the female's alimentary tract for production of symbiont capsules: MSM and SSM retain the symbiotic bacteria, SSM and EEM produce and supplement the PMDP-containing secretion to the symbiotic bacteria, and EEM excretes

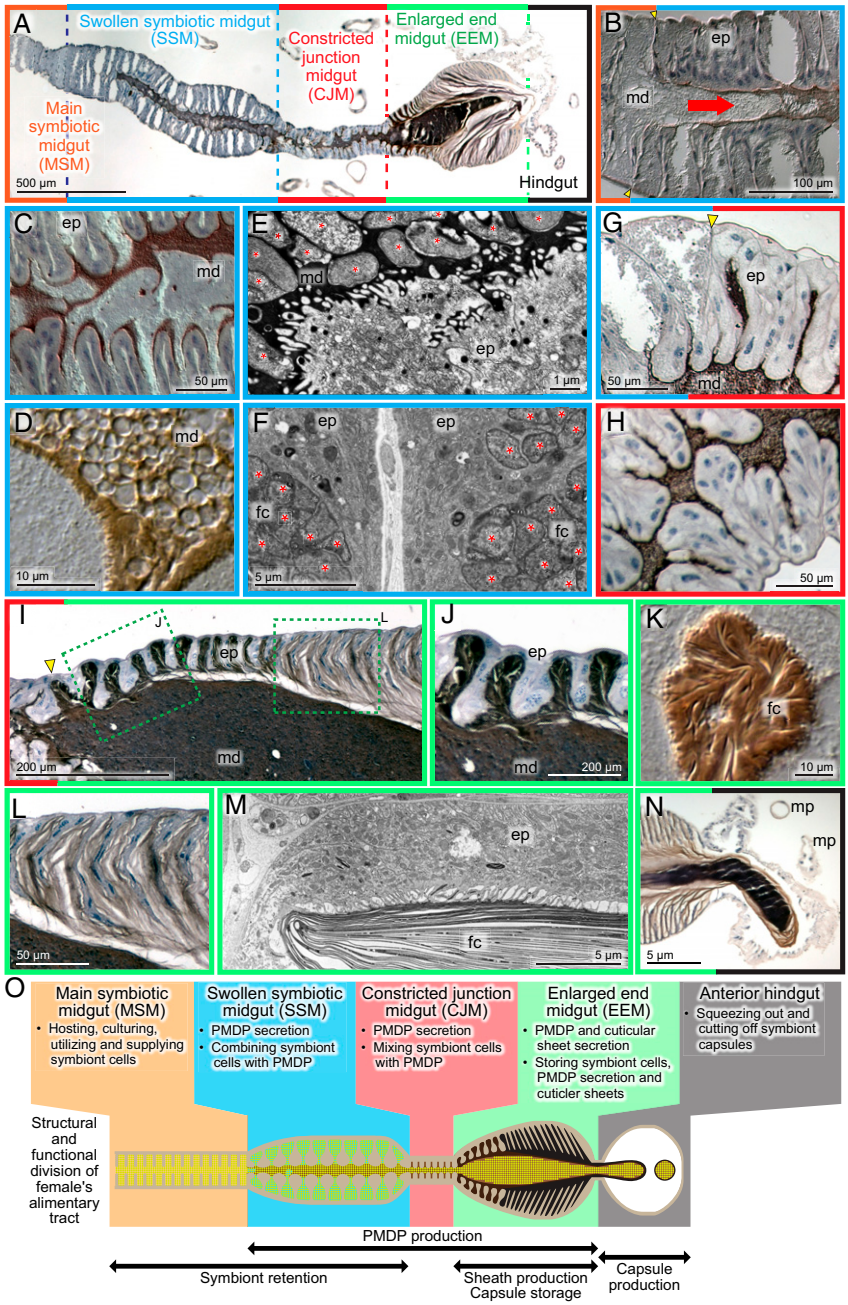

Fig. 2. Formation process of symbiont capsules in female's posterior midgut organs. (*A*) Whole sectioned image of the female's posterior midgut organs for production of symbiont capsules. Many microscopic images are combined to obtain the whole picture. PMDP is immunohistochemically visualized in dark brown, whereas cell nuclei are counterstained in purple. *Ishikawaella* cells are not stained but cytologically recognized. The morphologically and functionally differentiated regions, MSM, SSM, CJM (constricted junction midgut), EEM, and hindgut, are highlighted by different frame colors. (*B*) The MSM–SSM junction. The symbiont cells from MSM are combined with the PMDP-containing secretion from the epithelial cells of SSM. (*C*) Magnified image of the symbiont cells mixed with the PMDP-containing secretion in SSM. (*D*) Magnified differential interference contrast (DIC) image of the symbiont–secretion mixture in SSM, in which round symbiont cells are seen within the PMDP-positive secretion. (*E*) Transmission electron microscopic (TEM) image of the PMDP-secreting epithelium of SSM. Well-developed microvilli, electron-dense PMDP-containing secretion, and the symbiont cells (asterisks) are seen. (*F*) TEM image of the symbiont cells (asterisks) in the fold cavities of SSM. An outer space between the neighboring folds is seen at the center. (*G*) The SSM–CJM junction. (*H*) Magnified image of CJM, whose narrow inner cavity is filled with a homogeneous mixture of the symbiont cells and the PMDP-containing secretion. (*I*) The CJM–EEM junction. The upstream folds of EEM (highlighted in *J*) are wide, secreting much PMDP with cuticular sheets, whereas the downstream folds of EEM (highlighted in *L*) are narrow and deep, mainly secreting cuticular sheets with some PMDP. The main duct is voluminous, storing a large amount of the symbiont–secretion mixture. (*J*) Magnified image of the upstream folds of EEM, which secrete much PMDP with cuticular sheet. (*K*) Magnified DIC image of an upstream fold cavity of EEM. (*L*) Magnified image of the downstream folds of EEM from which cuticular sheets decorated with some PMDP are spreading out. (*M*) TEM image of a downstream fold of EEM. Secreted cuticular sheets in the fold cavity are seen. (*N*) EEM-hindgut junction in the process of capsule formation. A mass of the symbiont–secretion mixture surrounded by the cuticular shell is being squeezed out to form a symbiont capsule. (*O*) Structural and functional differentiation of the posterior intestinal regions for production of symbiont capsules in adult plataspid females. ep, epithelium or epithelial cell; fc, fold cavity; md, main duct; mp, Malpighian tubule. Yellow arrowheads indicate the border of the intestinal regions, whereas red arrows indicate the flow direction in the intestinal main duct.

the cuticular layered shell and stores the capsule components consisting of the symbiont–secretion mixture and the capsule shell. Passing through the serially arranged gut regions, the symbiotic bacteria are embedded in the PMDP-containing secretion and finally packaged into the symbiont capsules (Fig. 2 and *SI Appendix*, Fig. S2 and Note S1). Symbiont cytometry and in vitro culturing of the dissected gut regions with ^{15}N-labeled glutamine revealed that the symbiont's metabolic activities are high in MSM, low in SSM, and almost undetectable in EEM (Fig. 3), indicating that the symbiont cells are transformed into a dormant status during the capsule formation process.

PMDP Knockdown Stops Capsule Production. Considering the abundant supplementation and intimate packaging of PMDP with the symbiont cells in the symbiont capsules, some important biological functions were suspected for the protein. Hence, we performed RNA interference (RNAi) knockdown of PMDP expression. When adult females were injected with double-stranded RNA (dsRNA) representing a partial PMDP gene region (see *SI Appendix*, Fig. S1*B*), the PMDP gene expression was suppressed by two orders of magnitude within 3 d, and the suppression continued for over 2 wk (*SI Appendix*, Fig. S3*A*). The RNAi knockdown of PMDP did not affect the number of the eggs, the clutch size of the egg masses, and the hatch rate of the eggs (*SI Appendix* and Fig. 3 *B*–*D*) but drastically suppressed the capsule production. Upon laying egg masses, the control adult females deposited around one capsule per three eggs, where the capsules were large

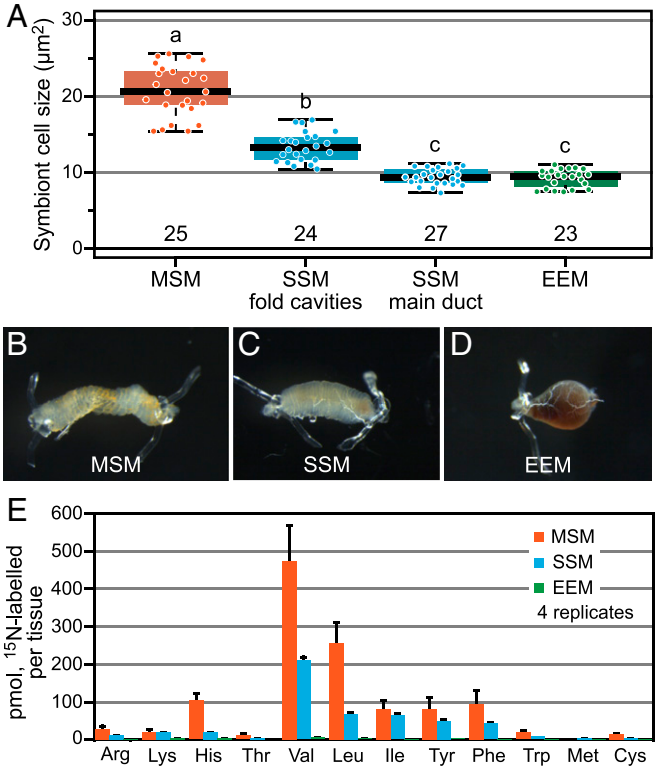

Fig. 3. Symbiont morphology and metabolism during capsule formation process. (*A*) Symbiont cell sizes in MSM, in the fold cavity of SSM, in the main duct of SSM, and in EEM measured on transmission electron microscopic images. Different letters (a, b, and c) indicate statistically significant differences (Tukey HSD test; $P < 0.05$). (*B*–*D*) Ligated and dissected preparations of MSM (*B*), SSM (*C*), and EEM (*D*) for the metabolic measurement. (*E*) Metabolic activity of symbiont cells evaluated by synthesis of essential and semi-essential amino acids, which was analyzed by in vitro culturing and LC-MS of dissected MSM, SSM, and EEM in the presence of ^{15}N-glutamine. Averages and SEs of four replicate assays are shown.

in size and dark in color, throughout the experimental period for 2 wk (Fig. 4 *A*, *Top* and Fig. 4 *B*–*D* and Movie S1). By contrast, the PMDP-knockdown females started to produce abnormal capsules, which were smaller in size and paler in color, around 7 d after dsRNA injection (Fig. 4 *A*, *Middle*). Coincidently, the number of capsules started to decline (Fig. 4 *B* and *C*). Subsequently, size and number of the capsules became smaller and smaller. Around 18 d after dsRNA injection and on, no or only a few tiny translucent capsules were produced by the PMDP-knockdown females (Fig. 4 *A*, *Bottom* and Fig. 4 *B* and *C*). These females laid eggs normally but deposited few capsules, thereby producing the egg masses devoid of the symbiont capsules (Fig. 4*E* and Movie S2).

PMDP Knockdown Causes Symbiont Degeneration. Detailed histological inspection of the midgut organs provided insight into how and why the PMDP-knockdown females stopped producing the symbiont capsules. The dark-colored material in the main tract of SSM and the whole EEM, which represented the capsule components produced and stored in these organs, disappeared following the PMDP dsRNA injection (Fig. 4*F*, "Dissected capsule-producing midgut" column). On the day of dsRNA injection as well as in the control insects, the symbiont cells were morphologically normal; in the fold cavities of SSM, the symbiont cells were densely packed, whereas in the main tract of SSM and within EEM, the symbiont cells were embedded in the PMDP-containing secretion (Fig. 4*F*, "0 day after injection" row). Three days after dsRNA injection, the PMDP-containing secretion decreased, and the symbiont cells looked degenerate in the main duct of SSM and in EEM (Fig. 4*F*, "3 days after injection" row). Two weeks after dsRNA injection, the PMDP-containing secretion almost disappeared in SSM and EEM, and the symbiont cells were highly degenerate in the main duct of SSM and completely disintegrated in EEM (Fig. 4*F*, "14 days after injection" row). It is notable that, deep in the fold cavities of SSM where little PMDP was secreted, the symbiont degeneration was not conspicuous (Fig. 4*F*, "Fold cavity" column), suggesting a connection between the PMDP depletion and the symbiont degeneration.

PMDP Knockdown Disrupts Symbiont Transmission, Affects Nymphal Behavior, and Retards Nymphal Growth. How does the maternal RNAi knockdown of PMDP, which causes symbiont degeneration and arrested capsule production, affect the next generation of the host insect? The eggs laid by the PMDP-knockdown females hatched normally, like the eggs laid by the control females (*SI Appendix*, Fig. S3*D*). However, the hatchlings exhibited strikingly different behaviors between the treatment groups. The newborn nymphs from the egg masses of the control females immediately sucked the symbiont capsules for around 1 h and then aggregated and became quiescent near the eggshells as previously reported (19) (Fig. 5*A* and Movie S3). By contrast, the newborn nymphs from the egg masses of the PMDP-knockdown females became neither aggregated nor quiescent but wandered around and dispersed (Fig. 5*B* and Movie S4). Plausibly, the nymphs could not acquire the symbiotic bacteria from the egg masses without intact symbiont capsules and thus continued to search for them. This idea was supported by quantification of symbiont titers in the nymphal insects. From the egg masses with normal dark capsules (Fig. 4 *A*, *Top*), the nymphs acquired considerable titers of the symbiotic bacteria, which were comparable to the symbiont titers in the control nymphs (Fig. 5 *C*, *Left*). From the egg masses with small pale capsules (Fig. 4 *A*, *Middle*), the nymphs acquired very low levels of the symbiotic bacteria in comparison with the symbiont titers in the control nymphs (Fig. 5 *C*, *Middle*). From the egg masses with no or a few tiny translucent capsules (Fig. 4 *A Bottom*), the nymphs acquired no symbiotic bacteria (Fig. 5 *C*, *Right*). In accordance with the symbiont transmission failure, the nymphs from the egg masses

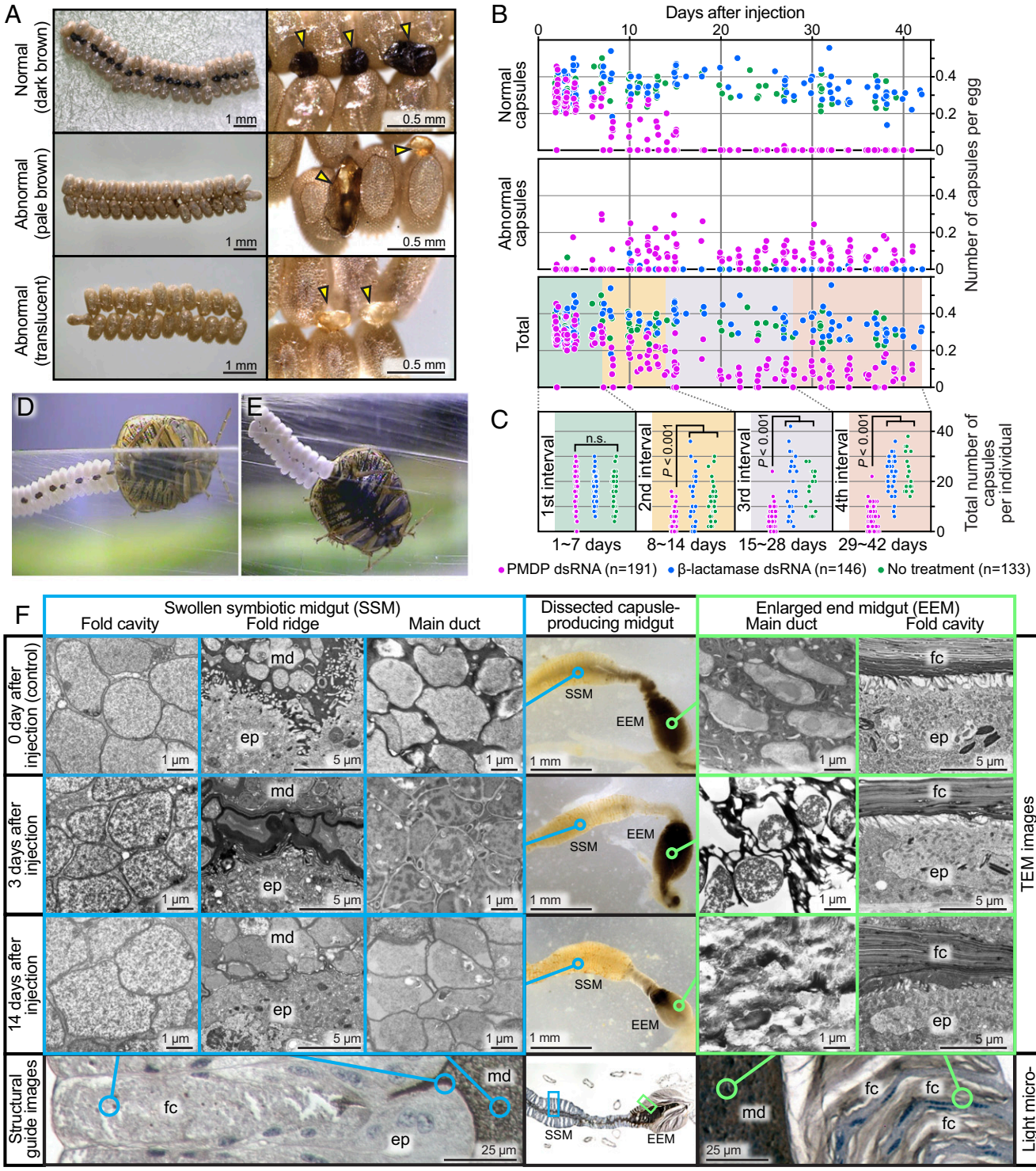

Fig. 4. Effects of PMDP RNAi on capsule production and symbiotic bacteria. (*A*) Egg masses and symbiont capsules produced by PMDP-knockdown females: top row, a control egg mass, with normal capsules dark brown in color; middle row, an egg mass produced about 10 d after PMDP dsRNA injection, with abnormal small pale capsules; bottom row, an egg mass produced about 20 d after PMDP dsRNA injection, with abnormal tiny translucent capsules; left column, underside images of whole egg masses; and right column, magnified images of symbiont capsules indicated by arrowheads. (*B*) Time course of arrested capsule production in PMDP-knockdown females: (*Top*) number of normal capsules per egg; (*Middle*) number of abnormal capsules per egg; and (*Bottom*) total number of capsules per egg. Each colored symbol indicates an egg mass: magenta, egg masses laid by PMDP dsRNA-injected females; blue, egg masses laid by β-lactamase dsRNA-injected control females; and green, egg masses laid by control females without dsRNA injection. (*C*) Statistical test for arrested capsule production in PMDP-knockdown females. From left to right are shown the data of 1 to 7, 8 to 14, 15 to 28, and 29 to 42 d after injection, in which the number of capsules was significantly suppressed by PMDP dsRNA injection except for the first interval (1 to 7 d) (Tukey HSD test, $P < 0.001$). n.s., not significant. (*D*) A control female laying an egg mass with symbiont capsules. Also see Movie S1. (*E*) A PMDP-knockdown female laying an egg mass devoid of symbiont capsules. Also see Movie S2. (*F*) Effects of PMDP RNAi on symbiotic bacteria and PMDP-containing secretion in the capsule-producing midgut organs. ep, epithelial cell; fc, fold cavity; md, main duct.

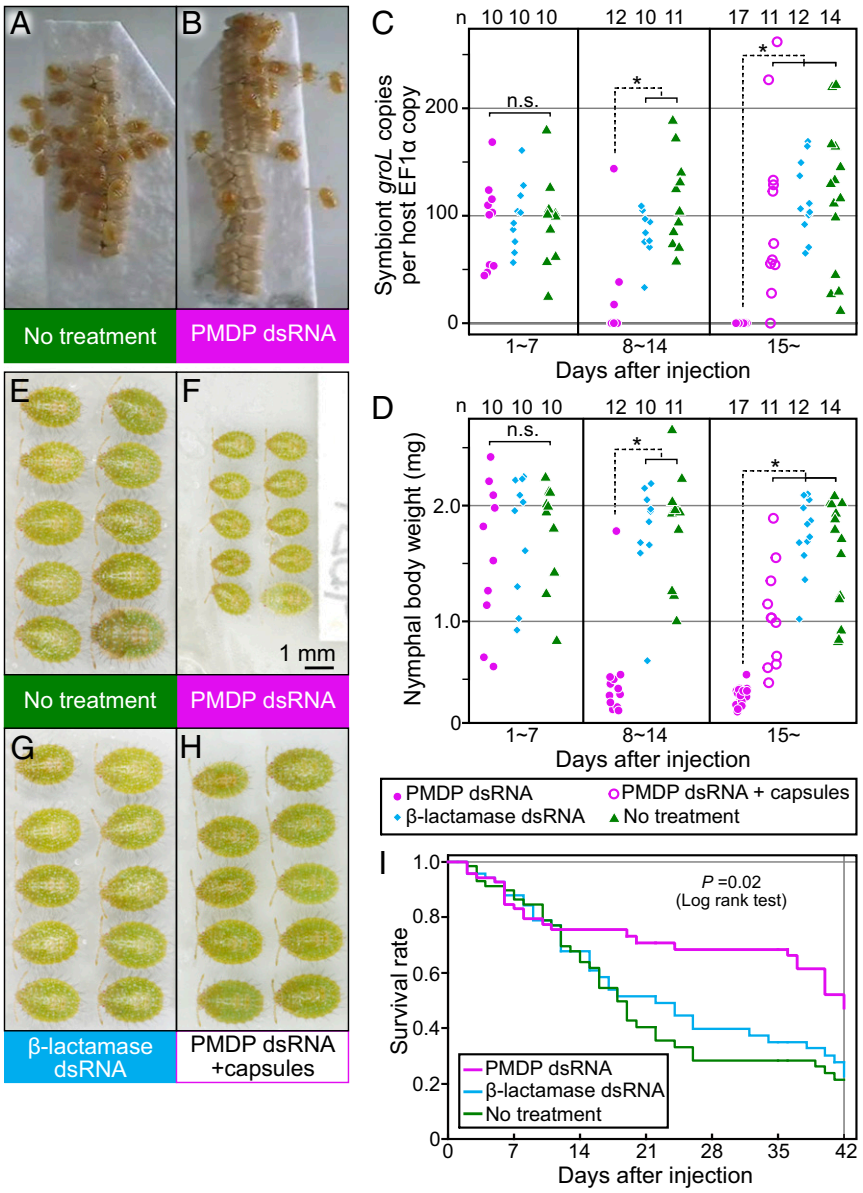

Fig. 5. Effects of PMDP RNAi on nymphal phenotypes and maternal survival. (*A*) Newborn nymphs from a control egg mass, quiescently aggregating near the eggshells. Also see Movie S3. (*B*) Newborn nymphs from an egg mass laid by a PMDP dsRNA-injected female, wandering around and dispersing from the eggshells. Also see Movie S4. (*C*) Symbiont titers in 16-d-old nymphs. Each colored symbol represents a nymph: magenta, offspring of PMDP dsRNA-injected mothers; blue, offspring of β-lactamase dsRNA-injected control mothers; green, offspring of noninjected control mothers; and open magenta, offspring of PMDP dsRNA-injected mothers artificially supplemented with normal symbiont capsules. Asterisks show statistically significant differences (Tukey HSD test; $P < 0.01$). (*D*) Wet body weights of 16-d-old nymphs. Abbreviations are the same as in *C*. (*E*–*H*) Photographs of the 16-d-old nymphs. Magenta (*E*), green (*F*), blue (*G*), and open magenta (*H*) reflect the symbols in *C* and *D*. (*I*) Trade-off between maternal survival and capsule production. Survival curves of adult females are shown: magenta, PMDP dsRNA-injected females; blue, β-lactamase dsRNA-injected control females; and green, no injection control females. PMDP dsRNA-injected females exhibited a significantly higher survival rate (log rank test, $P = 0.02$; n.s., not significant).

laid by the PMDP-knockdown females exhibited drastic growth retardation (Fig. 5 *D*–*G*). Notably, when the egg masses devoid of the symbiont capsules laid by the PMDP-knockdown females were experimentally supplemented with normal symbiont capsules, the nymphs restored symbiont acquisition and growth (Fig. 5 *C*, *D*, and *H*). These results indicate that RNAi knockdown of PMDP causes symbiont degeneration and arrested capsule production, which disrupt vertical transmission of the essential symbiont and, consequently, result in fatal fitness defects of the offspring.

Trade-Off between Capsule Production and Maternal Survival. Notably, the experimental adult females exhibited intriguing mortality patterns. While the control females died almost constantly throughout the experimental period, the PMDP-knockdown females stopped dying around 10 d after dsRNA injection (Fig. 5*I*), which was coincidental with the timing of when the capsule production started to decline in the PMDP-knockdown females (Fig. 4*B*). The significantly lower mortality of the PMDP-knockdown females in comparison with the control females continued until around 36 d after dsRNA injection (Fig. 5*I*). These patterns suggest that the capsule production may incur substantial cost for the egg-laying females. In other words, the reproductive females are producing the symbiont capsules for their offspring at the expense of their own survival, which highlights a significant parent–offspring trade-off mediated by investment in successful vertical transmission of the genome-eroded symbiont.

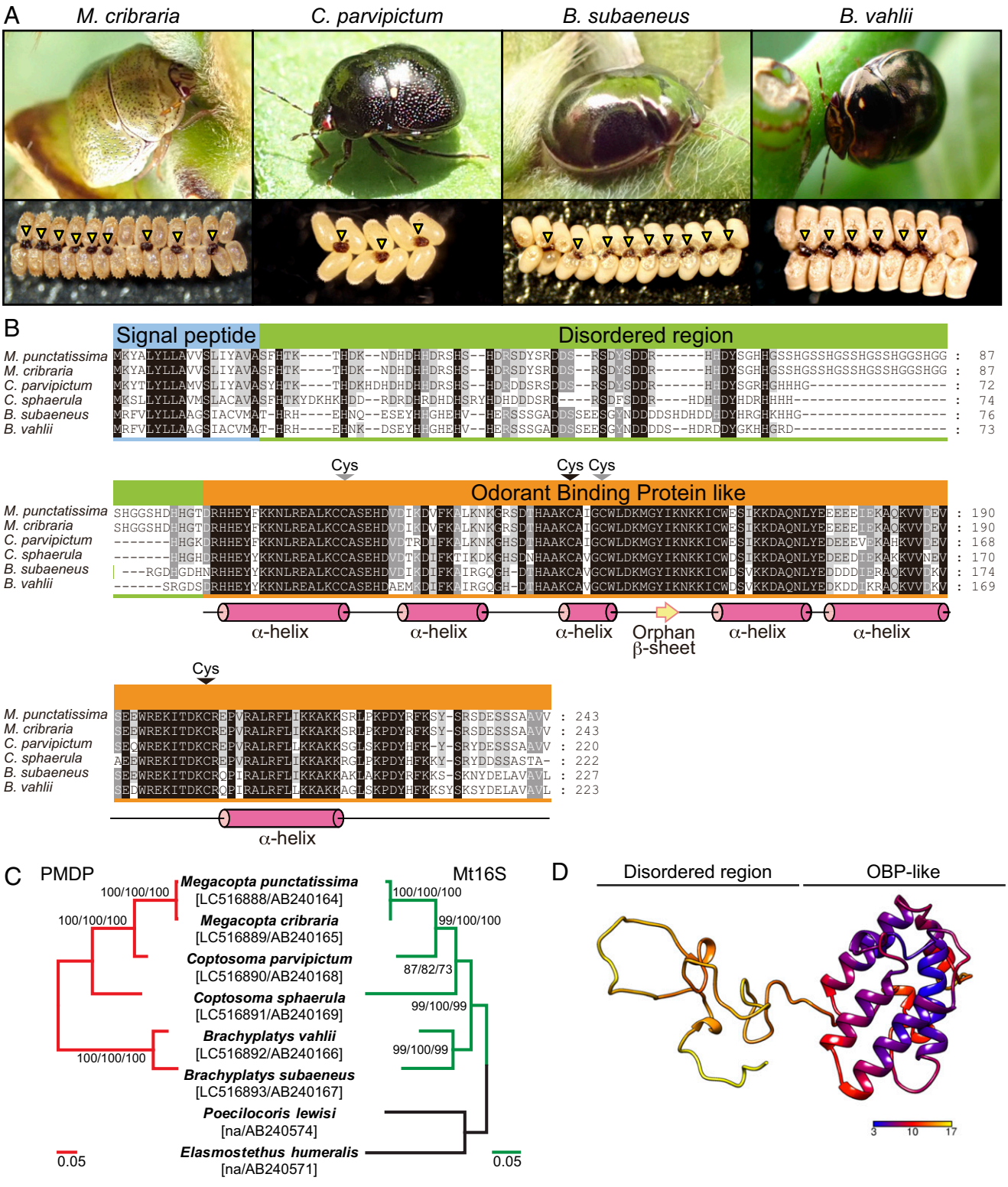

Fig. 6. Molecular, structural, and evolutionary features of PMDP. (*A*) Various plataspid stinkbugs (*Top*) and their symbiont capsules (*Bottom*, arrowheads). (*B*) Aligned PMDP sequences of six plataspid species representing three genera. In the OBP-like region, deduced secondary structures including six α-helices are shown at the bottom, whereas four conserved cysteine residues are depicted at the top. (*C*) Comparison of PMDP phylogeny and mitochondrial phylogeny. Maximum likelihood phylogenies inferred from 712 aligned nucleotide sites of PMDP and 1,501 aligned nucleotide sites of mitochondrial 16S ribosomal RNA gene are shown. Support probabilities are indicated at each node in the order of maximum likelihood/maximum parsimony/neighbor-joining. Sequence accession numbers are in brackets. Note that the PMDP phylogeny is unrooted due to the absence of appropriate outgroup sequences. (*D*) A structural model for PMDP predicted by C-QUARK (24). Colors indicate the average prediction errors: 3, blue; 10, red; and 17, yellow.

Evolutionary Origin of PMDP. All stinkbug species of the family Plataspidae thus far examined were reported to deposit symbiont capsules upon oviposition (12, 20), which was also confirmed by our observation in this study (Figs. 1 *A* and *B* and 6*A*). Meanwhile, no other stinkbug groups exhibit such a peculiar trait of symbiont capsule production (21, 22). When and how, then, has PMDP evolved in the evolutionary course of plataspid stinkbugs? A comparison of PMDP sequences among six plataspid species representing three genera showed that the N-terminal signal peptide region and the C-terminal OBP-like region were conserved, whereas the disordered region was not (Fig. 6*B*). The PMDP phylogeny and the mitochondrial gene phylogeny exhibited perfect congruence in topology (Fig. 6*C*), which strongly suggests that PMDP was acquired by the common ancestor of extant plataspid species and has evolved in parallel with speciation and diversification of the Plataspidae. The computational structural calculation of PMDP predicted the OBP-like region as a globular domain consisting of six α-helices, typical of OBPs (23), and the disordered region as a polypeptide stretch without a fixed three-dimensional structure (24) (Fig. 6*D*). The OBP-like region of PMDP exhibited some sequence similarity (<36% for amino acid sequences) to OBP-like sequences of other insects, including the stinkbugs in the databases. Meanwhile, the disordered region of PMDP yielded no significant hits, and no OBP-like sequences from other insects including stinkbugs accompanied a stretch of the PMDP-like disordered polypeptide. These observations suggest that PMDP is a newly evolved OBP-like protein that acquired an extra disordered segment in the lineage of the Plataspidae. Many OBP-like genes were identified in the transcriptomic/genomic data of the plataspid stinkbugs and other stinkbug species (*SI Appendix*, Fig. S4 and Table S2), illustrating the dynamic evolution of OBP-allied multigene families as observed in *Drosophila* and other insects (25, 26). While conventional OBPs were reported to function in antennae, bind to small hydrophobic odorant/pheromone molecules, and mediate chemosensory perception, most OBPs and allied proteins are not restricted to olfactory tissues and probably involved in

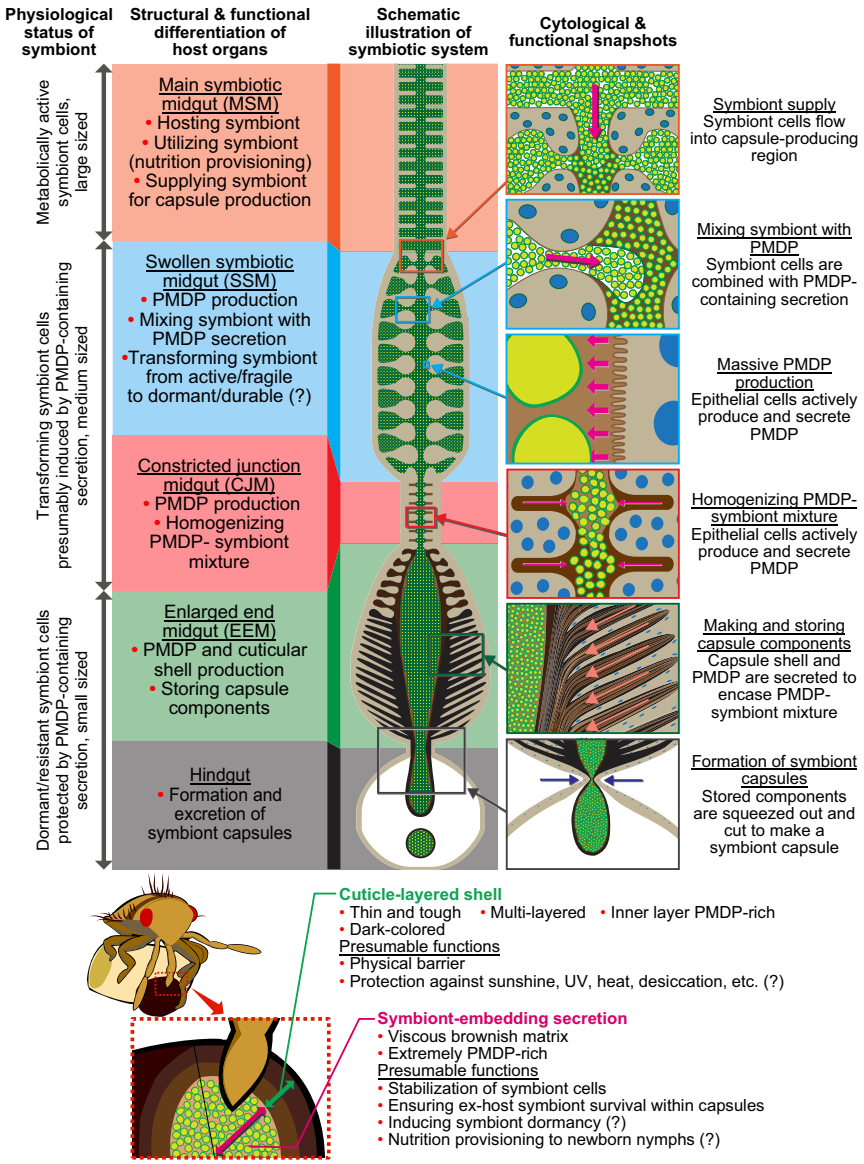

Fig. 7. Biological functions of PMDP and female-specific posterior midgut regions during the process of capsule production and vertical symbiont transmission.

hitherto unknown biological functions (23, 26). In this context, the symbiosis-related function of PMDP mediated by microbial interactions uncovers a previously unknown biological aspect of OBP-like proteins and highlights potential functional versatility of the OBP-allied multigene families.

Conclusion and Perspective

In conclusion, PMDP is a host's secretion protein essential for survival outside the host and successful vertical transmission of the genome-reduced symbiont. Fig. 7 graphically summarizes what molecular, cellular, metabolic, and morphological specializations are involved in the elaborate processes for maintenance and transformation of the symbiotic bacteria, production, and supplementation of the PMDP-containing secretion, formation, and shaping of the symbiont capsules and vertical symbiont transmission to the next generation. Evolutionarily, PMDP was acquired by the host's common ancestor via co-option of a specific lineage of the OBP-allied multigene families for the symbiosis-related, novel biological function. The discovery of the host factor underpinning the gut microbial association should be of general relevance, considering the biological importance of gut microbiome across the animal kingdom, including humans (27–30). A survey of analogous functional molecules in other systems could lead to a deeper understanding of symbiosis. The mode of action of PMDP for enabling the symbiont survival outside the host is still to be established. We speculate that PMDP may bind to the symbiont surface and stabilize the fragile bacterial cell, which should be verified by biochemical and microbiological experiments using purified or recombinant PMDP protein. Besides PMDP, minor proteinous and other capsule ingredients may also have important biological roles, which deserve future studies. The evolutionary origin of the symbiont capsule as well as the female-specific capsule-producing organ is still an enigma. The stinkbug family Plataspidae embraces some 530 species and 56 genera in the world (31), and a wider survey of the world's plataspid diversity would shed further light on the origin and evolution of PMDP and the symbiont capsule. Finally, we point out the possibility that mass production of PMDP and an understanding of its molecular function would lead to novel approaches to cultivation and/or preservation of fastidious microorganisms (7, 32).

Materials and Methods

Laboratory-maintained strains and wild-caught individuals of the common plataspid stinkbug *M. punctatissima* were mainly used in this study. The laboratory strains were reared on soybean plants (*Glycine max*), pea pods (*Pisum sativum*), or kidney bean pods (*Phaseolus vulgaris*) at 25 °C under a long-day condition of 16 h light and 8 h dark. The field-collected insects were either immediately used for experiments, preserved in an ultracold freezer at −80 °C until use, or reared as described above during experiments. *M. punctatissima* and other plataspid stinkbugs used in this study are listed in *SI Appendix*, Table S3. More detailed methods are described in *SI Appendix, SI Materials and Methods*.

Data Availability. Nucleotide sequence data have been deposited in DNA DataBank of Japan (PMDP gene sequences, LC516888–LC516893 (33); RNAseq reads, DRX227360–DRX227374 (34); OBP-like gene sequences, ICQY01000001–ICQY01000008, ICQX01000001–ICQX01000016, ICQW01000001–ICQW01000004, and ICQV01000001–ICQV01000024) (35). All other study data are included in the article and/or supporting information.

ACKNOWLEDGMENTS. We thank Ehab Abouheif and Hassan Salem for comments on the manuscript and Mariko Taguchi for technical assistance. This study was supported by the Japan Society for the Promotion of Science KAKENHI Grant JP25221107 to T.F. and the Japan Science and Technology Agency ERATO Grants JPMJER1803 and JPMJER1902 to T.F.

1. M. McFall-Ngai *et al.*, Animals in a bacterial world, a new imperative for the life sciences. *Proc. Natl. Acad. Sci. U.S.A.* **110**, 3229–3236 (2013).
2. S. F. Gilbert, T. C. G. Bosch, C. Ledón-Rettig, Eco-evo-devo: Developmental symbiosis and developmental plasticity as evolutionary agents. *Nat. Rev. Genet.* **16**, 611–622 (2015).
3. J. I. Perlmutter, S. R. Bordenstein, Microorganisms in the reproductive tissues of arthropods. *Nat. Rev. Microbiol.* **18**, 97–111 (2020).
4. J. P. McCutcheon, N. A. Moran, Extreme genome reduction in symbiotic bacteria. *Nat. Rev. Microbiol.* **10**, 13–26 (2011).
5. J. P. McCutcheon, B. M. Boyd, C. Dale, The life of an insect endosymbiont from the cradle to the grave. *Curr. Biol.* **29**, R485–R495 (2019).
6. G. M. Bennett, N. A. Moran, Heritable symbiosis: The advantages and perils of an evolutionary rabbit hole. *Proc. Natl. Acad. Sci. U.S.A.* **112**, 10169–10176 (2015).
7. F. Masson, B. Lemaitre, Growing ungrowable bacteria: Overview and perspectives on insect symbiont culturability. *Microbiol. Mol. Biol. Rev.* **84**, e00089-20 (2020).
8. M. A. Fares, M. X. Ruiz-González, A. Moya, S. F. Elena, E. Barrio, Endosymbiotic bacteria: groEL buffers against deleterious mutations. *Nature* **417**, 398 (2002).
9. S. L. Rutherford, Between genotype and phenotype: Protein chaperones and evolvability. *Nat. Rev. Genet.* **4**, 263–274 (2003).
10. M. Kupper, S. K. Gupta, H. Feldhaar, R. Gross, Versatile roles of the chaperonin GroEL in microorganism-insect interactions. *FEMS Microbiol. Lett.* **353**, 1–10 (2014).
11. N. Nikoh, T. Hosokawa, K. Oshima, M. Hattori, T. Fukatsu, Reductive evolution of bacterial genome in insect gut environment. *Genome Biol. Evol.* **3**, 702–714 (2011).
12. T. Hosokawa, Y. Kikuchi, N. Nikoh, M. Shimada, T. Fukatsu, Strict host-symbiont cospeciation and reductive genome evolution in insect gut bacteria. *PLoS Biol.* **4**, e337 (2006).
13. T. Fukatsu, T. Hosokawa, Capsule-transmitted gut symbiotic bacterium of the Japanese common plataspid stinkbug, *Megacopta punctatissima*. *Appl. Environ. Microbiol.* **68**, 389–396 (2002).
14. T. Hosokawa, Y. Kikuchi, X. Y. Meng, T. Fukatsu, The making of symbiont capsule in the plataspid stinkbug *Megacopta punctatissima*. *FEMS Microbiol. Ecol.* **54**, 471–477 (2005).
15. T. Hosokawa, Y. Kikuchi, T. Fukatsu, How many symbionts are provided by mothers, acquired by offspring, and needed for successful vertical transmission in an obligate insect-bacterium mutualism? *Mol. Ecol.* **16**, 5316–5325 (2007).
16. S. Shigenobu, H. Watanabe, M. Hattori, Y. Sakaki, H. Ishikawa, Genome sequence of the endocellular bacterial symbiont of aphids *Buchnera* sp. APS. *Nature* **407**, 81–86 (2000).
17. T. Ohbayashi *et al.*, Insect's intestinal organ for symbiont sorting. *Proc. Natl. Acad. Sci. U.S.A.* **112**, E5179–E5188 (2015).
18. S. Oishi, M. Moriyama, R. Koga, T. Fukatsu, Morphogenesis and development of midgut symbiotic organ of the stinkbug *Plautia stali* (Hemiptera: Pentatomidae). *Zoological Lett.* **5**, 16 (2019).
19. T. Hosokawa, Y. Kikuchi, M. Shimada, T. Fukatsu, Symbiont acquisition alters behaviour of stinkbug nymphs. *Biol. Lett.* **4**, 45–48 (2008).
20. P. Buchner, *Endosymbiosis of Animals with Plant Microorganisms* (Interscience, New York, 1965).
21. H. Salem, L. Florez, N. Gerardo, M. Kaltenpoth, An out-of-body experience: The extracellular dimension for the transmission of mutualistic bacteria in insects. *Proc. Biol. Sci.* **282**, 20142957 (2015).
22. T. Hosokawa, T. Fukatsu, Relevance of microbial symbiosis to insect behavior. *Curr. Opin. Insect Sci.* **39**, 91–100 (2020).
23. M. Tegoni, V. Campanacci, C. Cambillau, Structural aspects of sexual attraction and chemical communication in insects. *Trends Biochem. Sci.* **29**, 257–264 (2004).
24. W. Zheng *et al.*, Deep-learning contact-map guided protein structure prediction in CASP13. *Proteins* **87**, 1149–1164 (2019).
25. F. G. Vieira, A. Sánchez-Gracia, J. Rozas, Comparative genomic analysis of the odorant-binding protein family in 12 *Drosophila* genomes: Purifying selection and birth-and-death evolution. *Genome Biol.* **8**, R235 (2007).
26. F. G. Vieira, J. Rozas, Comparative genomics of the odorant-binding and chemosensory protein gene families across the Arthropoda: Origin and evolutionary history of the chemosensory system. *Genome Biol. Evol.* **3**, 476–490 (2011).
27. R. E. Ley, C. A. Lozupone, M. Hamady, R. Knight, J. I. Gordon, Worlds within worlds: Evolution of the vertebrate gut microbiota. *Nat. Rev. Microbiol.* **6**, 776–788 (2008).
28. P. Engel, N. A. Moran, The gut microbiota of insects–Diversity in structure and function. *FEMS Microbiol. Rev.* **37**, 699–735 (2013).
29. A. E. Douglas, Simple animal models for microbiome research. *Nat. Rev. Microbiol.* **17**, 764–775 (2019).
30. N. A. Moran, H. Ochman, T. J. Hammer, Evolutionary and ecological consequences of gut microbial communities. *Annu. Rev. Ecol. Evol. Syst.* **50**, 451–475 (2019).
31. L. Jessop, A review of the genera of Plataspidae (Hemiptera) related to *Libyaspis*, with a revision of *Cantharodes*. *J. Nat. Hist.* **17**, 31–62 (1983).
32. S. S. Epstein, The phenomenon of microbial uncultivability. *Curr. Opin. Microbiol.* **16**, 636–642 (2013).
33. R. Koga, DDBJ accession nos. LC516888–LC516893. DNA Databank of Japan. http://getentry.ddbj.nig.ac.jp/getentry/na/LC516888. Deposited 22 January 2020.
34. M. Moriyama, DRA accession nos. DRX227360–DRX227374. DNA Databank of Japan. https://ddbj.nig.ac.jp/DRASearch/query?acc=DRX227360. Deposited 1 July 2020.
35. N. Nikoh, DDBJ accession nos. ICQY01000001–ICQY01000008, ICQX01000001–ICQX01000016, ICQW01000001–ICQW01000004, and ICQV01000001–ICQV01000024. DNA Databank of Japan. http://getentry.ddbj.nig.ac.jp/getentry/na/ICQY01000001. Deposited 21 August 2020.